

Optical and magneto-optical FIR properties of bilayer graphene

D.S.L. Abergel and Vladimir I. Fal'ko

Physics Department, Lancaster University, Lancaster, LA1 4YB, UK

We analyse the spectroscopic features of bilayer graphene determined by the formation of pairs of low-energy and split bands in this material. We show that the inter-Landau-level absorption spectrum in bilayer graphene at high magnetic field is much denser in the FIR range than that in monolayer material, and that the polarisation dependence of its lowest energy peak can be used to test the form of the bilayer ground state in the quantum Hall effect regime.

Graphene (atomic mono- and bilayer of graphite) [1, 2, 3] is a gapless two-dimensional (2D) semiconductor [5, 6]. When used in transistor-type devices, the density and type (n or p) of carriers in it can be controlled using the underlying gate [1], which has been exploited in the recent studies of the quantum Hall effect (QHE) in such structures. The sequencing of QHE plateaux in graphene [1, 2, 3] revealed the peculiar properties of the charge carriers in this material: Dirac-type chiral electrons with Berry phase π in monolayers [4, 5], and the Berry phase 2π chiral quasiparticles [6] and doubled degeneracy of the zero-energy Landau level (LL) in bilayers.

The electromagnetic (EM) field absorption in graphene at zero magnetic field has already been studied [7, 8, 9, 10, 11]. While the DC conductivity of monolayer graphene increases linearly with the carrier density [1, 12], the real part of its high-frequency conductivity [7, 9] is independent of the electron density in a wide spectral range above the threshold $\hbar\omega > 2|\epsilon_F|$, which determines a featureless absorption coefficient $g_1 = \pi e^2/\hbar c$. In contrast, the bilayer absorption coefficient,

$$g_2 = (2\pi e^2/\hbar c) f_2(\omega), \quad (1)$$

reflects the presence and dispersion of two pairs of bands in this material [6, 8, 15, 16]. In this Letter, we analyse far-infrared (FIR) magneto-optical properties due to the inter-LL [6, 13] transitions in bilayer graphene and compare them to those in monolayer material. The low-energy part of the absorption spectrum in a bilayer subjected to a strong magnetic field is much denser than that of a monolayer, reflecting the parabolic dispersion of its low-energy bands, with the lowest FIR absorption peak formed by transitions involving one of two degenerate LLs at zero energy. Although the high-energy part of the bilayer absorption spectrum is not sensitive to the polarisation of FIR irradiation, below we show that its lowest peak may be strongly polarised reflecting the occupancy of the degenerate LLs in a bilayer determined by the form of its ground state in the QHE regime.

The electronic Fermi line in graphene surrounds the corners [14] \mathbf{K}_\pm of the hexagonal Brillouin zone [5] (where we set $\epsilon = 0$). In monolayer graphene, quasiparticles near the centres of valleys \mathbf{K}_\pm can be described by 4-component Bloch functions $\psi = [\phi_{\mathbf{K}_+A}, \phi_{\mathbf{K}_+B}, \phi_{\mathbf{K}_-B}, \phi_{\mathbf{K}_-A}]$ and the Hamiltonian $\hat{H}_1 = \xi v \sigma \cdot \mathbf{p}$, where

$\sigma = (\sigma_x, \sigma_y)$ are Pauli matrices acting in the space of electronic amplitudes on the two crystalline sublattices (A and B), $\xi = \pm$ in \mathbf{K}_\pm distinguishes between valleys, momentum $\mathbf{p} = -i\hbar\nabla - \frac{e}{c}\mathbf{A}$ is calculated with respect to the center of the corresponding valley and $\nabla \times \mathbf{A} = B\mathbf{1}_z$.

Bilayer graphene is composed of two coupled monolayers (with sublattices A, B and \tilde{A}, \tilde{B} in the bottom and top layer respectively) arranged according to Bernal stacking [5]: sites B of the honeycomb lattice in the bottom layer lie below \tilde{A} of the top layer. It also has a hexagonal Brillouin zone with two inequivalent valleys, but carries twice the number of electronic dispersion branches which can be found using the next-neighbour hopping Hamiltonian [6] acting in the space of sublattice states $[\phi_{\mathbf{K}_+A}, \phi_{\mathbf{K}_+\tilde{B}}, \phi_{\mathbf{K}_+\tilde{A}}, \phi_{\mathbf{K}_+B}; \phi_{\mathbf{K}_-A}, \phi_{\mathbf{K}_-\tilde{B}}, \phi_{\mathbf{K}_-B}, \phi_{\mathbf{K}_-\tilde{A}}]$,

$$\hat{H}_2 \approx \begin{pmatrix} \xi v_3 \sigma^t \cdot \mathbf{p} & \xi v \sigma \cdot \mathbf{p} \\ \xi v \sigma \cdot \mathbf{p} & \gamma_1 \sigma_x \end{pmatrix}. \quad (2)$$

Here, v is determined by the AB ($\tilde{A}\tilde{B}$) intra-layer hopping, γ_1 is the strongest inter-layer $\tilde{A}B$ hopping element, and $v_3 \ll v$ is due to a direct weak hop between AB sublattices. Note that $\sigma_{x,y,z}^t$ are transposed matrices. Equation (2) determines two types of branches in the electronic spectrum of graphene [6, 15] observed in the recent ARPES studies [16]: split-bands,

$$\epsilon_s^\pm = \pm(\gamma_1/2)[\sqrt{1 + 4v^2p^2/\gamma_1^2} + 1], \quad (3)$$

formed by symmetric and antisymmetric states based upon $\tilde{A}B$ sublattices and two the gapless branches, ϵ_c^\pm . For $\epsilon \gg \epsilon_L \equiv \frac{1}{2}\gamma_1(v_3/v)^2$, the dispersion in gapless branches can be approximated by

$$\epsilon_c^\pm = \pm(\gamma_1/2)[\sqrt{1 + 4v^2p^2/\gamma_1^2} - 1]. \quad (4)$$

For $|\epsilon| < \frac{1}{4}\gamma_1$, gapless bands are formed by states from sublattices A and \tilde{B} described using the 4-component Bloch functions $\chi = [\phi_{\mathbf{K}_+A}, \phi_{\mathbf{K}_+\tilde{B}}, \phi_{\mathbf{K}_-\tilde{B}}, \phi_{\mathbf{K}_-A}]$ and the reduced low-energy Hamiltonian [6, 17],

$$\hat{H}_2 = -\frac{1}{2m_2}(\sigma \cdot \mathbf{p})\sigma_x(\sigma \cdot \mathbf{p}) + \delta\hat{H}_w + \frac{\beta p^2}{m_2}; \quad (5)$$

$$\delta\hat{H}_w = \xi v_3 \sigma^t \cdot \mathbf{p}; \quad m_2 = \gamma_1/2v^2, \quad |\beta| \ll 1.$$

Here $m_2 \approx 0.055m_e$ and the last term in \hat{H}_2 takes into account the weak AA and BB intra-layer hopping [18].

In a 2D electron gas with conductivity $\sigma(\omega) \ll c/2\pi$, absorption of an EM field $\mathbf{E}_\omega = \ell E e^{-i\omega t}$ with polarisation ℓ [$\ell_\oplus = \sqrt{\frac{1}{2}}[\mathbf{l}_x - i\mathbf{l}_y]$ for right- and $\ell_\ominus = \sqrt{\frac{1}{2}}[\mathbf{l}_x + i\mathbf{l}_y]$ for left-hand circularly polarised light arriving along the direction antiparallel to a magnetic field] can be characterised by the absorption coefficient $g \equiv E_i E_j^* \sigma_{ij}(\omega)/S$: the ratio between Joule heating and the energy flux $\mathbf{S} = c\mathbf{E} \times \mathbf{H}/4\pi = -S\mathbf{l}_z$ transported by the EM field. Using the Keldysh technique, we express

$$g = \frac{8e^2}{c\omega} \Re \int \frac{F d\epsilon}{N} \widehat{\text{Tr}} \left\{ \hat{v}_i \ell_i \hat{G}^R(\epsilon) \hat{v}_j \ell_j^* \hat{G}^A(\epsilon + \omega) \right\},$$

where $\hat{\mathbf{v}} = \partial_{\mathbf{p}} \hat{H}$ is the velocity operator, $\widehat{\text{Tr}}$ includes the summation both over the sublattice indices “tr” and over single-particle orbital states, N is the normalisation area of the sample and $F = n_F(\epsilon) - n_F(\epsilon + \omega)$ takes into account the occupancy of the initial and final states. Here we have included spin and valley degeneracy.

For a 2D gas in a zero magnetic field, the electron states are weakly scattered plane waves. Using the plane wave basis and the matrix form of the bilayer Hamiltonian $\hat{\mathcal{H}}_2$, we express the retarded/advanced Greens functions of electrons in the bilayer as $\hat{G}^{R/A}(\mathbf{p}, \epsilon) = [\epsilon \pm \frac{1}{2}i\hbar\tau^{-1} - \hat{H}_2(\mathbf{p})]^{-1}$ and $\widehat{\text{Tr}} = \int d^2\mathbf{p} \frac{N}{(2\pi\hbar)^2} \text{tr}$. After neglecting the renormalisation of the current operator by vertex corrections at $\omega\tau \gg 1$ and the momentum transfer from light (since $v/c \sim 3 \times 10^{-3}$), we reproduce [7, 9] the constant absorption coefficient $g_1^\parallel = \pi e^2 \hbar c$ ($f_1 = \frac{1}{2}$) in monolayer graphene and arrive at the expression for the absorption coefficient of a bilayer for light polarised in the plane of graphene sheet [21]:

$$g_2^\parallel = \frac{2\pi e^2}{\hbar c} f_2(\Omega), \quad \Omega \equiv \frac{\hbar\omega}{\gamma_1} > \frac{2|\epsilon_F|}{\gamma_1}, \quad (6)$$

$$f_2 = \frac{\Omega + 2}{2(\Omega + 1)} + \frac{\theta(\Omega - 1)}{\Omega^2} + \frac{(\Omega - 2)\theta(\Omega - 2)}{2(\Omega - 1)},$$

where $\theta(x < 0) = 0$ and $\theta(x > 0) = 1$. The above result agrees with the calculation by J. Nilsson *et al* [8] taken in the clean limit and $T=0$. The frequency dependence [19] of the bilayer optical absorption is illustrated in Fig.1, where an additional structure in the vicinity of $\hbar\omega = \gamma_1$ ($\gamma_1 \approx 0.4\text{eV}$ [5, 16]) is due to the electron-hole excitation between the low-energy band ϵ_c^\pm and the split band ϵ_s^\pm . For the higher photon energies, $\hbar\omega \gtrsim 2\gamma_1$, the frequency dependence almost saturates at $f \approx 1$. Over the entire spectral interval shown in Fig.1, the absorption coefficient for the left- and right-handed light are the same, so that Eq. (6) is applicable [21] to light linearly polarised in the graphene plane.

High-field FIR magneto-optics of graphene. In a magnetic field, the continuous zero-field spectrum, Eq. (6)

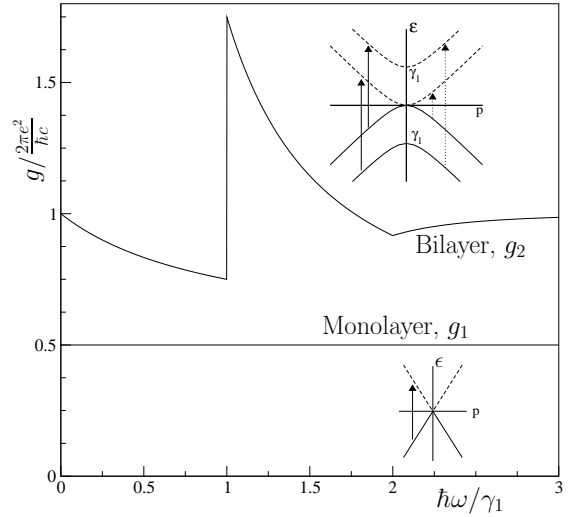


FIG. 1: Absorption coefficient of bilayer and monolayer graphene in the optical range of frequencies. Insets illustrate the quasiparticle dispersion branches in the vicinity of ϵ_F and possible optical transitions.

splits into lines determined by transitions between Landau levels. The LLs can be studied after rewriting \hat{H}_1 and $\hat{\mathcal{H}}_2$ in terms of descending, $\pi = p_x + ip_y$ and raising, $\pi^\dagger = p_x - ip_y$ operators in the basis of Landau functions $\varphi_{n \geq 0}$, leading to $\sigma \cdot \mathbf{p} = \begin{pmatrix} 0 & \pi^\dagger \\ \pi & 0 \end{pmatrix}$. The resulting monolayer spectrum [13] contains 4-fold degenerate ($2 \times$ spin and $2 \times$ the valley index) states: one at $\epsilon_0 = 0$ with $\psi_{0K_+} = [\varphi_0, 0, 0, 0]$ and $\psi_{0K_-} = [0, 0, \varphi_0, 0]$, and pairs of levels $\epsilon_{n\pm} = \pm \hbar v \lambda_B^{-1} \sqrt{2n}$ ($\lambda_B = \sqrt{\hbar c / eB}$ is the magnetic length) with $\psi_{n\pm, K_+} = \frac{1}{\sqrt{2}}[\varphi_n, \mp i\varphi_{n-1}, 0, 0]$ and $\psi_{n\pm, K_-} = \frac{1}{\sqrt{2}}[0, 0, \varphi_n, \mp i\varphi_{n-1}]$. We neglect the electron spin splitting and use the index $\alpha = \pm$ in $\epsilon_{n\alpha}$ and $\psi_{n\alpha, K}$ for the conduction (+) and valence (-) band LLs.

The bilayer spectrum features [6] a group of 8 states with $\epsilon_0 \approx \epsilon_1 \approx 0$: $\chi_{0K_+} = [\varphi_0, 0, 0, 0]$, $\chi_{0K_-} = [0, 0, \varphi_0, 0]$ and $\chi_{1K_+} = [\varphi_1, 0, 0, 0]$, $\chi_{1K_-} = [0, 0, \varphi_1, 0]$ (4×2 , due to spin degeneracy), and a ladder of almost equidistant 4-fold degenerate levels $\epsilon_{n\pm} = \pm \hbar\omega_c \sqrt{n(n-1)}$ ($2 \times$ spin and $2 \times$ the valley index) with $\hbar\omega_c = \hbar^2 / m_2 \lambda_B^2$ and wave functions $\chi_{n\pm, K_+} = \frac{1}{\sqrt{2}}[\varphi_n, \pm \varphi_{n-2}, 0, 0]$, $\chi_{n\pm, K_-} = \frac{1}{\sqrt{2}}[0, 0, \varphi_n, \pm \varphi_{n-2}]$. The latter result can be found from the analysis of the first term in the low-energy-band Hamiltonian \hat{H}_2 , which dominates for $|\epsilon| < \frac{1}{4}\gamma_1$ and high magnetic fields such that $\lambda_B^{-1} > \gamma_1 v_3 / v^2$. Numerical diagonalisation of the full \hat{H}_2 and $\hat{\mathcal{H}}_2$ shows [6] that this degeneracy is not lifted by the warping term $\delta\hat{H}_w$, and also the above-described grouping of LLs in bilayer graphene was confirmed in the recent QHE measurements [3]. It has been noticed [17] that degenerate levels with $n = 0$ (χ_{0K_+}, χ_{0K_-}) and $n = 1$ (χ_{1K_+}, χ_{1K_-}) can be weakly split by the second-

neighbour hopping term $\beta p^2/m_2$, to $\varepsilon_0 = \frac{\beta}{2}\hbar\omega_c$ and $\varepsilon_1 = \frac{3\beta}{2}\hbar\omega_c$, where $\beta \ll 1$ [18]. However, it is more likely that, at a high magnetic field, electrons in an ideally clean bilayer with filling factor $-4 < \nu < 4$ would form a correlated ground state in which the occupancy of $n = 0$ and 1 LLs would be determined by the electron-electron interaction. The correlated ground state is particularly interesting in a bilayer with $\nu = 0$, where 2D electrons can form a ferromagnetic QHE state in which both $n = 0$ and 1 states are half-filled, or an antiferromagnetic state with one fully occupied and one empty LL. Below we show that these two ground states can be distinguished experimentally on the basis of magneto-absorption spectra measured in a circularly polarised FIR light.

Figure 2(a) illustrates selection rules for the inter-LL transitions in bilayer and monolayer graphene. In both cases, photons with the in-plane [21] polarisation ℓ_{\ominus} are absorbed via transitions where the LL index changes as $n \rightarrow n - 1$ ($n \geq 1$), whereas absorption of ℓ_{\oplus} photons happens via transitions $n \rightarrow n + 1$ ($n \geq 0$). Assuming the same broadening $\hbar\tau^{-1}$ of all LLs [22], we arrive at the following magneto-absorption spectra for monolayer [10] and bilayer graphene (for $\varepsilon_L < \hbar\omega < \frac{1}{4}\gamma_1$):

$$g_J^{\oplus/\ominus}(B, \omega) = \frac{2\pi e^2}{\hbar c} f_J^{\oplus/\ominus}(B, \omega), \quad (7)$$

$$f_1^{\ominus} = \sum_{\alpha\alpha'} \frac{\frac{w_1\tau}{\pi\hbar} \frac{2b_{n-1}^2}{\alpha\sqrt{n-1-\alpha'}\sqrt{n}} (\nu_{n,\alpha'} - \nu_{n-1,\alpha})}{\frac{w_1^2\tau^2}{\hbar^2} [\frac{\hbar\omega}{w_1} - \alpha\sqrt{n-1} + \alpha'\sqrt{n}]^2 + 1}$$

$$f_1^{\oplus} = \sum_{\alpha\alpha'} \frac{\frac{w_1\tau}{\pi\hbar} \frac{2b_n^2}{\alpha\sqrt{n+1-\alpha'}\sqrt{n}} (\nu_{n,\alpha'} - \nu_{n+1,\alpha})}{\frac{w_1^2\tau^2}{\hbar^2} [\frac{\hbar\omega}{w_1} - \alpha\sqrt{n+1} + \alpha'\sqrt{n}]^2 + 1}$$

$$f_2^{\ominus} = \sum_{\alpha\alpha'} \frac{\frac{4c_{n-1}^2}{\pi\omega_c\tau} \frac{(\nu_{n,\alpha'} - \nu_{n-1,\alpha})(n-1)}{\alpha\sqrt{n^2-n-\alpha'}\sqrt{(n-1)(n-2)}}}{[\frac{\omega}{\omega_c} - \alpha\sqrt{n^2-n} + \alpha'\sqrt{(n-1)(n-2)}]^2 + \frac{\tau^{-2}}{\omega_c^2}}$$

$$f_2^{\oplus} = \sum_{\alpha\alpha'} \frac{\frac{4c_n^2}{\pi\omega_c\tau} \frac{(\nu_{n,\alpha'} - \nu_{n+1,\alpha})n}{\alpha\sqrt{n^2+n-\alpha'}\sqrt{n^2-n}}}{[\frac{\omega}{\omega_c} - \alpha\sqrt{n^2+n} + \alpha'\sqrt{n^2-n}]^2 + \frac{\tau^{-2}}{\omega_c^2}}.$$

Here $w_1 = \sqrt{2}\hbar v\lambda_B^{-1}$ and $\hbar\omega_c = \hbar^2/m_2\lambda_B^2$ are the characteristic energy scales for the LL spectra in monolayer ($J = 1; \varepsilon_{n\alpha}$) and bilayer ($J = 2; \varepsilon_{n\alpha}$) graphene, respectively, and $\alpha, \alpha' = \pm$ determine whether the corresponding state belongs to the conduction (+) or valence (-) band. Also, $\nu_{n,\alpha}$ are the filling factors of the corresponding LLs, and $b_0 = 1$, $b_{n \geq 1} = 1/\sqrt{2}$ for a monolayer and $c_{0,1} = 1$, $c_{n \geq 2} = 1/\sqrt{2}$ for the bilayer.

The denser magneto-absorption spectrum in bilayer graphene (as compared to the monolayer) is one of its features illustrated in Fig.2 (b). Another feature is that the intensity of the lowest absorption peak measured at the filling factor $\nu = 0$ may differ for ℓ_{\oplus} and ℓ_{\ominus} polarisations, reflecting the form of the ground state of a bilayer. Since

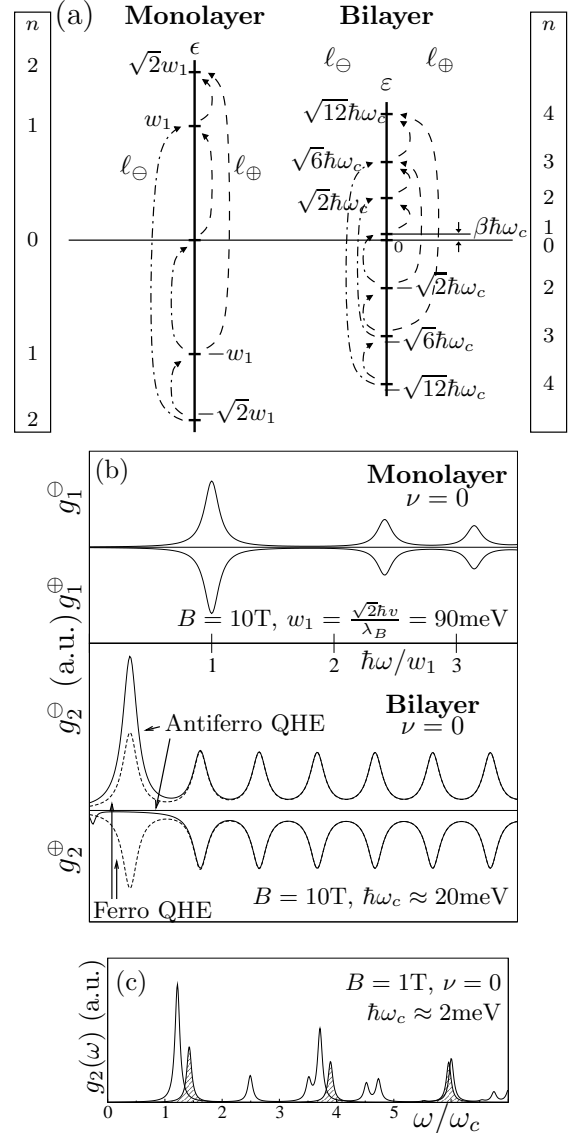


FIG. 2: (a) Allowed inter-LL transitions without trigonal warping effects. Dashed and dash-dot lines indicate transitions in ℓ_{\oplus} and ℓ_{\ominus} polarisations respectively. (b) Monolayer (top) and bilayer (bottom) FIR absorption spectra in ℓ_{\oplus} and ℓ_{\ominus} polarisations for $B = 10T$ and filling factor $\nu = 0$. Dashed and solid lines describe absorption by ferro- and antiferromagnetic states of the $\nu = 0$ bilayer. (c) Weak field, $B = 1T$, $\nu = 0$ magnetoabsorption in bilayer graphene with $\nu = 0$ calculated with ($v_3 = 0.2\nu$; dashed) and without ($v_3 = 0$, shaded) warping term in the Hamiltonian.

transitions from/to the $n = 0$ LL with $\varepsilon_0 \approx 0$ to/from the states $\varepsilon_{n\pm}$ with $n \geq 2$ are forbidden, the intensity and polarisation of the peak at $\omega = \sqrt{2}\omega_c$ are determined by transitions from/to $n = 1$ LL (also with $\varepsilon_1 \approx 0$) and directly reflect its occupancy. If the bilayer ground state is ferromagnetic, with a half-filled $n = 1$ LL, the absorption peak at $\omega = \sqrt{2}\omega_c$ will have the same intensity in both ℓ_{\oplus} and ℓ_{\ominus} polarisations. In contrast, absorption

by a $\nu = 0$ bilayer with antiferromagnetic ground state would contain this line only in one polarisation: in ℓ_{\ominus} if $n = 1$ LL is empty (fully occupied $n = 0$ LL) and in ℓ_{\oplus} if $n = 1$ LL is full. For comparison, the lowest peak in the spectrum of a monolayer with $\nu = 0$ appears in both polarisations, since both transitions to ($\epsilon_{1-} \rightarrow \epsilon_0$) and from ($\epsilon_0 \rightarrow \epsilon_{1+}$) half-filled $n = 0$ monolayer LL are possible. All higher-energy absorption peaks which involve transitions between filled valence band states ($\alpha = -$) and empty states in the conduction band ($\alpha = +$) have equal strengths in both polarisations.

One can test the selection rules shown in Fig. 2(a) using gated graphene structures [1, 2, 3]. By filling the monolayer sheet with electrons up to $\nu = 2$ (a completely filled $n = 0$ LL), one would suppress the intensity of the lowest absorption peak in ℓ_{\ominus} polarisation and double its size in the polarisation ℓ_{\oplus} . By depleting the monolayer to $\nu = -2$ state (emptying the $n = 0$ LL) one would achieve the opposite effect. Similarly, in a bilayer with a completely filled pair of degenerate $\epsilon_0 \approx \epsilon_1 \approx 0$ LLs which takes place at $\nu = 4$, light with $\omega = \sqrt{2}\omega_c$ can be absorbed only in the ℓ_{\oplus} polarisation. By depleting the bilayer down to $\nu = -4$ one could suppress the absorption in this line in ℓ_{\oplus} polarisation while retaining ℓ_{\ominus} absorption. Also, note that a weak transition between $n = 0$ and 1 LLs with a low frequency $\beta\omega_c$ (microwave range) is possible, to the measure of a small β and depending on the LL filling.

Finally, the warping term $\delta\hat{H}_w$ in Eq. (5) mixes each state $\chi_{n\alpha,K}$ with states $\chi_{(n\pm 3)\alpha,K}$. This generates weak transitions (with the coefficient $\delta g_2 \sim (v_3 m_2 \lambda_B / \hbar)^2 g_2$) between states which are 2 and 4 levels apart. Although such transitions are negligibly weak at high fields where the first term in \hat{H}_2 is dominant, they become relevant at weak fields, where $\lambda_B^{-1} \lesssim \gamma_1 v_3 / v^2$, and the low-frequency absorption spectrum of a bilayer acquires an additional structure. In Fig. 2(c) we compare the absorption spectra in a $\nu = 0$ bilayer [22] at $B = 1$ T calculated numerically for $v_3 = 0$ and $v_3 = 0.2v$.

In *conclusion*, we have described peculiar optical and FIR magneto-optical properties of bilayer graphene. The zero field optical absorption spectrum shown in Fig. 1 reflects the existence of four bands in the electronic spectrum of this material whereas the FIR magneto-optical spectrum of bilayer graphene, which is much denser than that of a monolayer, reflects the parabolic dispersion of its low-energy bands ϵ_c^{\pm} . Due to the interband character of the inter-LL transitions in graphene with low carrier density, the magneto-optical spectrum in a monolayer and the higher energy part of the bilayer spectrum ($\omega > 3\omega_c$) do not depend on the FIR light polarisation. However, the absorption peak at $\omega = \sqrt{2}\omega_c$ may appear differently in ℓ_{\oplus} and ℓ_{\ominus} polarised light, depending on the occupancy of the two zero-energy LL ($n = 0$ and 1) in bilayer graphene [3, 6]. In such spectroscopic studies, the weakness of g_2 can be overcome using the transport

detection of FIR absorption in the QHE regime.

We thank E.McCann and A.Varlamov for discussions and the EPSRC grant EP/C511743 for support.

-
- [1] K. Novoselov *et al*, Nature **438**, 197 (2005); Science **306**, 666 (2004)
- [2] Y. Zhang *et al*, Phys. Rev. Lett. **94**, 176803 (2005); Nature **438**, 201 (2005)
- [3] K. Novoselov *et al*, Nature Physics **2**, 177 (2006)
- [4] Y. Zheng, T. Ando, Phys. Rev. B **65**, 245420 (2002); V. Gusynin, S. Sharapov, Phys. Rev. Lett. **95**, 146801 (2005); A. Castro Neto, F. Guinea, N. Peres, Phys. Rev. B **73**, 205408 (2006)
- [5] M. S. Dresselhaus and G. Dresselhaus, Adv. Phys. **51**, 1 (2002); T. Ando, J. Phys. Soc. Jpn. **74**, 777 (2005)
- [6] E. McCann and V.I. Fal'ko, Phys Rev. Lett. **96** 086805 (2006)
- [7] V. Gusynin, S. Sharapov, J. Carbotte, Phys. Rev. Lett. **96**, 256802 (2006); V. Gusynin and S. Sharapov, Phys. Rev. B **73**, 245411 (2006)
- [8] J. Nilsson, A.H. Castro Neto, F. Guinea and N.M.R. Peres, cond-mat/0604106
- [9] L. Falkovsky and A. Varlamov, cond-mat/0606800
- [10] M. Sadowski *et al*, cond-mat/0605739; A. Iyengar *et al*, cond-mat/0608364
- [11] J. Cserti, cond-mat/0608219
- [12] K. Nomura and A.H. MacDonald, Phys. Rev. Lett. **96**, 256602 (2006); T. Ando, J. Phys. Soc. Jpn. **75**, 074716 (2006); V. Cheianov and V.I. Fal'ko, cond-mat/0608228
- [13] J.W. McClure, Phys. Rev. **104**, 666 (1956)
- [14] Here, $\mathbf{K}_{\pm} = \pm(\frac{2}{3}\hbar a^{-1}, 0)$, a is the lattice constant.
- [15] C. Lu *et al*, Phys. Rev. B **73**, 144427 (2006); J. Nilsson *et al*, Phys. Rev. B **73**, 214418 (2006); M. Koshino, T. Ando, Phys. Rev. B **73**, 245403 (2006); F. Guinea, A. Castro Neto, N. Peres, Phys. Rev. B **73**, 245426 (2006); B. Partoens, F. Peeters, Phys. Rev. B **74**, 075404 (2006)
- [16] T. Ohta *et al*, Science **313**, 951 (2006)
- [17] E. McCann, Phys. Rev. B **74**, 161403 (2006)
- [18] The sign of β is not known, though one can estimate using bulk graphite parameters [5] that $|\beta| \lesssim 10^{-2}$.
- [19] For $\hbar\omega \ll \frac{1}{4}\gamma_1$ this result transforms into $f_2 = 1$ suggested by J.Cserti [11] for the microwave absorption in bilayer graphene. However one should be aware that Eq. (6) and conclusions of Ref. [11] cannot be applied to $\hbar\omega \lesssim \epsilon_L = \frac{1}{2}\gamma_1(v_3/v)^2 \sim 1\text{meV}$. At $\epsilon_F \approx \epsilon_L$, the warping term $\delta\hat{H}_w$ causes the Lifshitz transition [20] in the topology of the Fermi line (in each valley): from singly-connected at $\epsilon_F > \epsilon_L$ to four pockets at $\epsilon_F < \epsilon_L$.
- [20] A.A. Abrikosov, *Fundamentals of the Theory of Metals*, North-Holland 1988
- [21] In contrast to monolayer graphene, a weak absorption of light polarised perpendicular to the bilayer is possible. A perturbation $\sigma_z e E_z d/2$ distinguishes between the on-site energies in the top and bottom layers separated by spacing d , which leads to weak absorption $g_2^z = (2\pi e^2/\hbar c)f_2^z$,

$$f_2^z = a_z^2 \Omega \left[\frac{1}{\Omega+1} + \frac{\theta(\Omega-2)}{\Omega-1} \right], \quad \Omega \equiv \hbar\omega/\gamma_1;$$

$$f_2^z(B, \omega) = \frac{a_z^2}{\pi} \sum_{n \geq 2} \frac{\tau\omega}{\tau^2\omega_c^2 \left(\frac{\omega}{\omega_c} - 2\sqrt{n^2 - n} \right)^2 + 1}$$

where $a_z = \gamma_1 d / 2\hbar v \sim 10^{-1}$, and the magneto-absorption spectrum at $\hbar\omega < \frac{1}{4}\gamma_1$ involves $\varepsilon_{n-} \rightarrow \varepsilon_{n+}$ inter-LL transitions.

[22] For energy-dependent broadening one replaces τ^{-1} in the sum in Eq. (7) with $\tau_{n\alpha, n'\alpha'}^{-1} = \frac{1}{2}(\tau_{n\alpha}^{-1} + \tau_{n'\alpha'}^{-1})$.